Strain, Size, and Composition of InAs Quantum Sticks Embedded in InP Determined via Grazing Incidence X-Ray Anomalous Diffraction

A. Létoublon,[1] V. Favre-Nicolin,[1,2] H. Renevier,[1,2,*] M. G. Proietti,[3] C. Monat,[4] M. Gendry,[4] O. Marty,[5] and C. Priester[6]

[1]*Commissariat à l'Energie Atomique, Département de Recherche Fondamentale sur la Matière Condensée, SP2M/NRS, 17 rue des martyrs, 38054 Grenoble Cedex 9, France*

[2]*Université Joseph Fourier, BP 53, F-38041, Grenoble Cedex 9, France*

[3]*Departamento de Física de la Materia Condensada, Instituto de Ciencia de Materiales de Aragón, CSIC-Universidad de Zaragoza, calle Pedro Cerbuna 12, 50009 Zaragoza, Spain*

[4]*LEOM, UMR-CNRS 5512, Ecole Centrale de Lyon, 69134 Ecully, France*

[5]*LENAC, Université Lyon I, 69621 Villeurbanne, France*

[6]*Institut d'Electronique, de Microélectronique et de Nanotechnologie, département ISEN, 59652 Villeneuve d'Ascq, France*

(Received 24 September 2003; published 5 May 2004)

We have used x-ray anomalous diffraction to recover the model-independent Fourier transform (x-ray structure factor) of InAs quantum sticklike islands embedded in InP. The average height of the quantum sticks, as deduced from the width of the structure factor profile, is 2.54 nm. The InAs out-of-plane deformation, relative to InP, is 6.1%. Diffraction anomalous fine structure provides evidence of pure InAs quantum sticks. Finite difference method calculations reproduce well the diffraction data, and give the strain along the growth direction. The chemical mixing at interfaces is also analyzed.

DOI: 10.1103/PhysRevLett.92.186101 PACS numbers: 68.65.La, 61.10.Nz

Semiconductor band structure can be strongly modified by reducing the characteristic size down to a length scale comparable to the effective wavelength of the carriers, i.e., of the order of several nanometers, leading to discrete energy levels [1]. InAs quantum structures, such as quantum wires (QWrs), are of great interest for the new generation of integrated devices since their typical emission wavelengths are within the relevant telecommunications range (1.3–1.6 μm). InAs QWrs are grown by molecular beam epitaxy (MBE), via the Stranski-Krastanow growth mode, on (001) InP substrates. The InAs/InP lattice mismatch $[(a_{\mathrm{InAs}} - a_{\mathrm{InP}})/a_{\mathrm{InP}}]$ is about 3.2%. Recent studies [2] have shown that a strong stress anisotropy appears during the growth deposition leading to a higher stress along [110] than along $[1\bar{1}0]$. The stress is released first along [110] leading to the QWr formation. To be suitable for devices, the nanostructures are encapsulated or embedded in a superlattice. In addition, they must be homogeneous in size, shape, and composition, to provide well defined emission wavelengths. The knowledge of strain field, chemical gradients, and chemical mixing at the interface is of great importance to understand the growth dynamics as well as the electronic and optical properties of the nanostructures.

In the present Letter we show that the structure factor (i.e., the Fourier transform) of embedded InAs sticklike nanostructures can be directly extracted by means of grazing incidence anomalous x-ray diffraction. The structure factor can then be used to recover the average height and strain of the quantum sticks (QSs), to determine their composition and check the As/P exchange. Strain of buried nanostructures is not only related to composition (Vegards's law), but it also depends on size, morphology, and cap layer thickness. Then, tuning the x-ray energy near an absorption edge of atoms that belong to the nanostructures is a way to modify their scattering power and to enhance the chemical sensitivity of diffraction. Grenier *et al.* [3] demonstrated the interest of using the site selectivity of the grazing incidence diffraction anomalous fine structure (GI-DAFS) spectroscopy to determine strain and composition of uncapped InAs QWrs grown on InP. These authors measured anomalous diffraction, at a single point of the reciprocal space as a function of the energy, across the As K edge. They recorded diffraction anomalous fine structure (DAFS) data that give similar information to extended x-ray absorption fine structure. More recently, Magalhaes-Panagio *et al.* [4] and Schülli *et al.* [5] have reported the use of grazing incidence anomalous diffraction to study the Ge composition profile of freestanding Ge islands grown on top of Si substrate. In that case, isostrain scattering could be unambiguously associated to isostrain slices, above and parallel to the Si surface, belonging to the islands [6]. In the present work we have performed grazing incidence 2D mappings of the reciprocal space to recover a model-free Fourier transform of small size embedded InAs QSs. With respect to the previous works, we have used anomalous diffraction to study quite a challenging system: nano-objects having a small size, which are encapsulated and the x-ray scattering contribution of which is mingled with that of bulk InP, whatever the momentum transfer is. We have extracted the structure factor of the nanostructures and we interpret the results by means of finite difference method (FDM) calculations with inputs from transmission electron microscopy (TEM) images, showing the monolayer scale sensitivity of this technique.

The sample we studied consists of one layer of InAs sticklike islands covered with a 10 nm thick InP cap layer. It was obtained by optimization of the MBE growth parameters to minimize the As/P exchange and reduce the height dispersion of the InAs islands [7,8]. The width of photoluminescence peaks reveals a very good height homogeneity [9], as confirmed by TEM measurements. The InAs QSs obtained with a nominal deposition thickness of 4 monolayers (ML) are 50 to 200 nm long along the $[1\bar{1}0]$ direction [Fig. 1(a)]. As shown by TEM of the cross section, the QSs exhibit a truncated triangle side shape with typical width of 22.5 ± 0.12 nm and homogeneous height of 2.4 nm [Fig. 1(b)].

Grazing incidence anomalous diffraction intensity can be written in the frame of the distorted wave Born approximation [10,11],

$$I(\vec{Q}, E) \propto \|T_i(\alpha_i, E)\|^2 \|F_T(\vec{Q})\|^2 \times \{[\cos(\varphi_T - \varphi_A) + \beta f'_{\mathrm{As}}]^2 + [\sin(\varphi_T - \varphi_A) + \beta f''_{\mathrm{As}}]^2\}, \quad (1)$$

where F_T is a complex structure factor of phase φ_T which includes the overall contribution of nonanomalous atoms and the Thomson scattering of all anomalous atoms, $\beta = \|F_A\|/(f^0_{\mathrm{As}}\|F_T\|)$ where F_A is a complex structure factor of phase φ_A which includes the Thomson scattering of all anomalous atoms (i.e., As atoms). $\|T_i(\alpha_i, E)\|^2$ is the incidence transmittivity, and α_i is the incidence angle that is close to the critical angle α_c. In the following, as the exit angle is much larger than the critical angle, the exit transmittivity $\|T_f(\alpha_f, E)\|^2 = 1$ and the scattering length (≈ 100 nm) is much larger than the epilayer thickness. The As scattering factor writes $f_{\mathrm{As}} = f^0_{\mathrm{As}} + f'_{\mathrm{As}} + if''_{\mathrm{As}}$, where f'_{As} and f''_{As} are the real and imaginary resonant scattering of As atoms. Equation (1) shows that diffraction measurements at various energies (at least three) at the As K edge allow the recovery of the β ratio, the phase difference $\Delta\varphi = \varphi_T - \varphi_A$, and a quantity that is proportional to the F_T modulus. The knowledge of $\|F_A\|$ and $\Delta\varphi$ readily gives information about the average size and strain of the nanostructures and chemical mixing at interface.

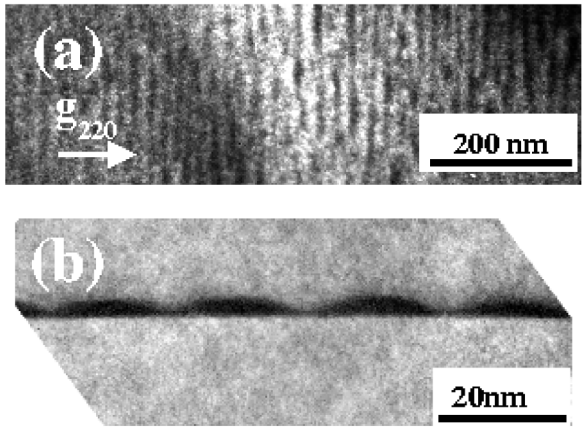

FIG. 1. Transmission electron microscopy images of InAs QSs embedded in InP (a) plane view and (b) cross section. One can clearly see the truncated triangle side shape.

Grazing incidence anomalous diffraction at the As K edge (11.867 keV) was performed at the French Collaborative Research Group beam lines BM32 and BM2 at the European Synchrotron Radiation Facility, using a Si(111) double crystal monochromator to select energies and mirrors to reject harmonics. Grazing incidence was used to minimize the substrate contribution. We recorded the scattering intensity in the vicinity of the (442) substrate reflection, at several energies across the As K edge. We chose a weak reflection ($h + k + l = 4n + 2$) for which the anomalous diffraction contrast is maximum; it lies in the mirror plane defined by the [110] and [001] directions to benefit from symmetry in the reciprocal space. Figure 2 shows the diffraction intensity map recorded at 11.840 keV and at a grazing incidence angle equal to the critical angle ($\alpha_i = \alpha_c = 0.2°$) to maximize the diffraction intensity. For that reflection the exit angle α_f is about 20°. A large amount of information can be drawn from such a map: the spreading of scattering in the [110] direction is due to both short range correlation and lattice strain in the corresponding direction in the real space ([110]), whereas in the [001] direction it is due to the sharp strain evolution. Figure 2 shows correlation satellites on both sides of the (442) reflection (S1 and S2); their positions relative to the substrate peak give a qualitative estimation of the mean correlation distance between the sticks. We find a value of 20.7 nm, that is in agreement with the TEM measurements.

The notable result in this map is the clear asymmetry of the S1 and S2 satellites; S1 exhibits a broad and twin

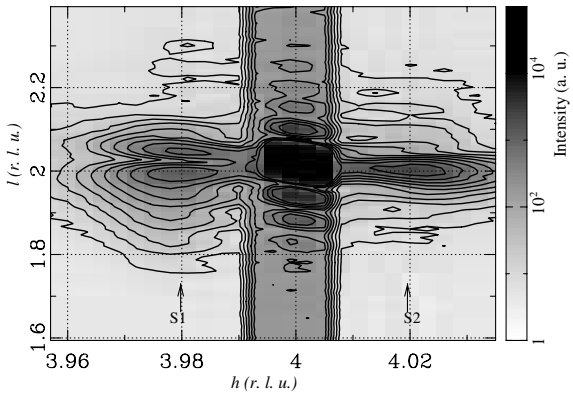

FIG. 2. Experimental diffraction map around the weak (442) reflection recorded at 11.840 keV in grazing incidence geometry ($\alpha_i = \alpha_c = 0.2°$, $\alpha_f \simeq 20°$), as a function of the reciprocal lattice unit (r.l.u.). The diffracted beam size at the sample position, as defined by the detector slits, was 5.5 mm long. S1 and S2 are correlation satellites due to the stick short range periodicity.

feature along the [001] direction, with a sharp splitting at $l = 2$, whereas S2 is a single feature centered approximately at $l = 2$. S1 corresponds to regions stretched along the [110] direction (tensile strain), i.e., to InAs sticks and InP regions located below and above the sticks. The peak S2, instead, corresponds to InP and InAs wetting layer regions that are compressed in between the sticks. Anomalous diffraction measurements at the As K edge show no intensity variations of satellite S2 as a function of energy, indicating that the InP contribution is the dominant one, as expected. This result leads to the conclusion that the transmittivity corrections can be neglected. Furthermore, our simulation shows that for a 1 ML thick wetting layer, the relative anomalous diffraction variation of peak S2 is about 4% and should have been detected. Thus, the wetting layer thickness should not exceed 1 ML .

Cutoff fringes are clearly observed in the l direction around the substrate Bragg peak position and give the total thickness of both the InAs QSs and the InP capping, that is equal to 11 ± 0.3 nm.

We performed l scans ($h = k = 3.98$) across the satellite S1, at nine different energies close to the As K edge including those corresponding to the minimum of f'_{As} and the white line of f''_{As}. A weak fluorescence background was subtracted and the data were normalized to l scans across the satellite S2, measured at the same energies. Then $F_A(\vec{Q})$, $F_T(\vec{Q})$, and $\Delta\varphi(\vec{Q})$ were extracted by fitting Eq. (1) to the energy dependent experimental intensities.

Figure 3(a) shows the experimental modulus of $F_A(\vec{Q})$, $F_T(\vec{Q})$. The QS's height average value ($\langle H \rangle$) can be estimated from the FWHM of F_A, $\langle H \rangle = c_{\mathrm{InP}}/[0.9 \times (\Delta F_A)_{\mathrm{FWHM}}] = 2.54$ nm, that is very near to the value measured by TEM.

Finite difference method simulations were performed to map the strain produced by InAs QSs embedded in InP and compare its Fourier transform to experimental diffraction intensity maps. We assumed a coherent growth of InAs on InP (supported by the lack of dislocations seen in TEM micrography). We performed finite difference method calculations [12], in a 2D periodic frame, in the plane determined by the [110] and [001] crystal axes, i.e., the wires have infinite length along $[1\bar{1}0]$ and a periodic structure along [110]. The QS's length is finite and rather short (50–200 nm), meaning 2D calculations slightly overestimate the strain, the relaxation along $[1\bar{1}0]$ not being permitted. We chose an FDM cell with a size of $(\sqrt{2}/4a)(a/4)$. Then, atoms were placed inside the crystallographic cell according to cubic face centered zinc blende structure, taking into account elastic deformation. Starting from atomic positions, diffraction intensity was calculated using the distorted wave Born approximation [10]. No structural disorder has been taken into account. The P and In anomalous scattering factors were obtained from theoretical values, whereas experimental values for As in bulk InAs were used.

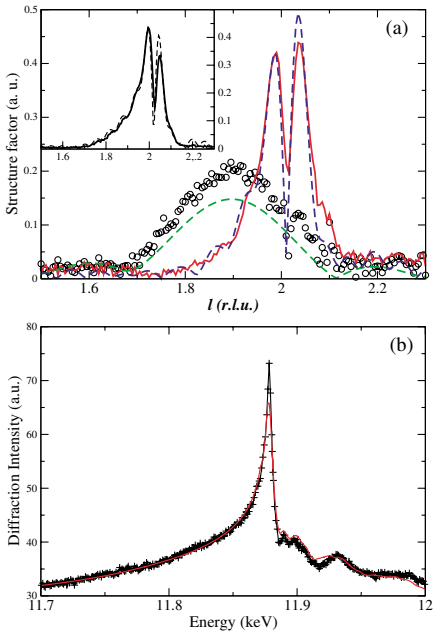

FIG. 3 (color online). (a) Experimental F_T (solid line) and F_A (open circles) modulus as a function of the r.l.u. l at $h = k = 3.98$ (across the satellite S1). F_A is the structure factor that corresponds to all anomalous atoms, i.e., As atoms only. Also shown are best simulation curves (dashed line) obtained with a FDM model made of pure InAs QSs with a truncated triangle side profile. The inset shows the experimental (solid line) and simulated (dashed line) square root of the diffraction intensity at 11.867 keV; at this energy, anomalous diffraction is maximized. (b) GI-DAFS spectrum recorded at the As K edge at the maximum of the F_A profile ($l = 1.9$) and the best fit curve obtained with pure InAs structure (solid line).

Figures 4(a) and 4(b) show the deformation maps with respect to InP lattice parameter, obtained with a model of embedded InAs QWrs as deduced from TEM images [Fig. 1(b)], that well reproduces the diffraction data. The QWrs side shape is a truncated triangle as shown by TEM. The total thickness of the QWrs and the capping is equal to 11 nm, as reported above. Figure 4(b) shows a map of deformations along the [001] direction (ε_{zz}), which emphasizes the morphology of the wires. Indeed the wires are compressed along [110] [with partial relaxation shown in Fig. 4(a)], thus expanded along [001]. This explains the sharp contrast of lattice strain shown in Fig. 4(b) (ε_{zz}). Figure 4(a) shows the relative strain ε_{xx} along [110]; here it is impossible to disentangle InAs from InP regions under and on the top of the wires, since the in-plane lattice strain is continuous at the interface. In Fig. 3(a) are shown the best calculated curves of F_A and F_T, obtained by optimizing the height of the wires, as well as As/P intermixing at the InAs/InP interface. The splitting of F_T is well reproduced by the simulation and is due to a scattering phase shift between InP cells above and below the wires. The overall wire thickness and width are found to be 9 ML and 22 nm, respectively. Note that

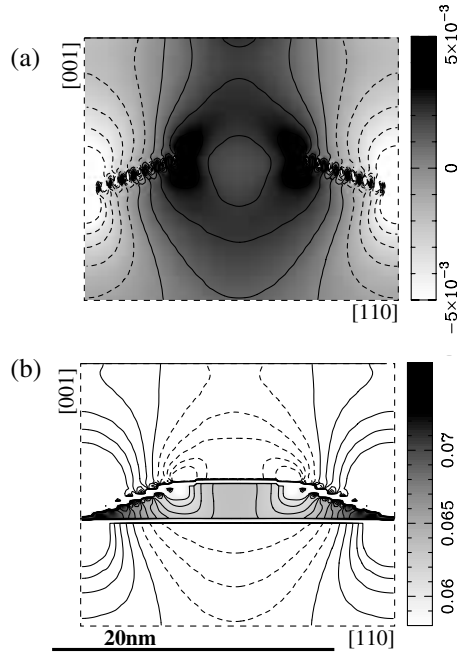

FIG. 4. FDM simulations of (a) $\varepsilon_{xx} = (a_{ij} - a_{\mathrm{InP}})/a_{\mathrm{InP}}$ and (b) $\varepsilon_{zz} = (c_{ij} - c_{\mathrm{InP}})/c_{\mathrm{InP}}$, where a_{ij} and c_{ij} are the parameters of cell (i, j). The strain is relative to bulk InP cell parameter; it is not the relative displacement. The ε_{zz} clearly show the morphology of InAs QWrs. Solid lines and dashed lines represent positive and negative contour strain, respectively, starting at -5×10^{-3} and spaced by 0.001. Ten additional ε_{zz} contours are shown inside the wire starting at 0.06. The solid line on top represents the sample surface.

FDM simulation well reproduces the relative positions of F_A and F_T, with a strain ε_{zz} of about 6.3% in the inner part of the wire. For comparison, the strain of a pseudomorphic InAs thin film grown on InP, as foreseen by the elastic theory, is 6.7%. The $\varepsilon_{zz} = (c - c_{\mathrm{InP}})/c_{\mathrm{InP}} = (l_{\mathrm{InP}} - l_{F_A})/l_{F_A}$ value, deduced directly from the reciprocal lattice position l_{F_A} of the maximum of F_A [Fig. 3(a)] is equal to $6.1 \pm 0.25\%$, i.e., within the uncertainty, equal to the value simulated by FDM. In order to determine the QS's composition and the local strain accommodation, grazing incidence diffraction anomalous fine structure spectrum was measured at the maximum of F_A ($h = k = 3.98$ and $l = 1.9$) at the As K edge. Figure 3(b) shows the experimental DAFS spectrum and the calculated curve obtained with the anomalous scattering factors f'_{As} and f''_{As} of bulk InAs. A scale factor, the detector efficiency as a function of the energy and the As occupation factor $(1 - x)$ inside the sticks were refined ($A_{1-x}P_x$). The best fit curve, shown in Fig. 3(b), corresponds to a value of $(1 - x)$ equal to 1.03 ($\beta = \|F_A\|/(f^0_{\mathrm{As}}\|F_T\|) = 0.12$, $\Delta\varphi = 159°$) , i.e., the QS's composition is pure InAs. GI-DAFS oscillations, in the energy range above the edge, will also give direct information on the local composition and on strain accommodation inside the sticks [3]. Detailed analysis of these oscillations will be reported elsewhere. The experimental curves (F_A and F_T) are compatible with a weak As/P intermixing at the InP interface, that would spread over 1 ML. Indeed, improving the signal-to-noise ratio together with a 2D data treatment would allow one to fully exploit the technique sensitivity to map the composition at the ML scale.

In conclusion, we have shown that anomalous diffraction can be used to extract the structure factor of small size InAs nanostructures *embedded* in InP matrix. This study is a first step towards a 2D and 3D analysis of anomalous diffraction maps and GI-DAFS data to recover the strain, size, shape, and composition of *embedded* nanostructures with a nondestructive probe giving access to the most complete structural information, that is very difficult to obtain otherwise.

We are very grateful to F. Né, J. S Micha, S. Arnaud, N. Boudet, B. Caillot, and J. F. Bérar for help during the experiments at the beam lines BM32 and BM2 at the ESRF. M. G. P. and H. R. acknowledge the support of Egide and Aciones Integradas Programmes (Grant No. HF2002-78) of the French and Spanish Ministries of Research and Education.

*Electronic address: Hubert.Renevier@cea.fr

[1] D. Bimberg, M. Grundman, and N. Ledensov, *Quantum Dot Heterostructures* (Wiley, Chistester, 1999).
[2] L. González, J. M. García, R. García, J. Martínez-Pastor, and C. Ballesteros, Appl. Phys. Lett. **76**, 1104 (2000).
[3] S. Grenier, M. Proietti, H. Renevier, L. Gonzalez, J. Garcia, and J. Garcia, Europhys. Lett. **57**, 499 (2002).
[4] R. Magalhaes-Panagio, G. Medeiros-Riberio, A. Malachias, S. Kycia, T. Kamins, and R. Stan, Phys. Rev. B **66**, 245312 (2002).
[5] T. Schülli, J. Stangl, Z. Zhong, R. Lechner, M. Sztucki, T. Metzger, and G. Bauer, Phys. Rev. Lett. **90**, 066105 (2003).
[6] I. Kegel, T. Metzger, A. Lorke, J. Peisl, J. Stangl, G. Bauer, K. Nordlund, W. Schoenfeld, and P. Petroff, Phys. Rev. B **63**, 035318 (2001).
[7] C. Monat, M. Gendry, J. Brault, M. Besland, P. Regreny, G. Hollinger, B. Salem, J. Olivares, G. Bremond, and O. Marty, in *Proceedings of the 14th Indium Phosphide and Related Materials Conference, IPRM'02, Stockholm, 2002* (IEEE, Piscataway, NJ, 2002), p. 565.
[8] M. Gendry *et al.*, J. Appl. Phys. **95**, 4761 (2004).
[9] B. Salem, T. Benyattou, G. Guillot, C. Bru-Chevallier, G. Bremond, C. Monat, G. Hollinger, and M. Gendry, Phys. Rev. B **66**, 193305 (2002).
[10] H. Dosch, *Critical Phenomena at Surfaces and Interfaces* (Springer-Verlag, Berlin, 1992).
[11] M. Proietti, H. Renevier, J. Hodeau, J. Garcia, J. Bérar, and P. Wolfers, Phys. Rev. B **59**, 5479 (1999).
[12] Y. Niquet, C. Priester, C. Gourgon, and H. Mariette, Phys. Rev. B **57**, 14 850 (1998).